

Order–Disorder Transitions in Block Copolymer Thin Films Studied by Guided Wave Depolarized Light Scattering with Grating Couplers

Jeffrey D. Wilbur,[†] Zhuangxi Fang,^{*,§} Bruce A. Garetz,^{*,‡,§} Maurice C. Newstein,^{||} and Nitash P. Balsara^{*,†,⊥}

Department of Chemical Engineering, University of California, Berkeley, California 94720; Department of Chemical and Biological Sciences and Othmer-Jacobs Department of Chemical and Biological Engineering, Polytechnic University, Six Metrotech Center, Brooklyn, New York 11201; Department of Electrical Engineering, Polytechnic University, Six Metrotech Center, Brooklyn, New York 11201; and Materials Sciences Division and Environmental Energy Technologies Division, Lawrence Berkeley National Laboratory, University of California, Berkeley, California 94720

Received November 20, 2007; Revised Manuscript Received March 1, 2008

ABSTRACT: We demonstrate the use of guided wave depolarized light scattering (GWDLS) with diffraction gratings for studying the properties of soft block copolymer films in the vicinity of order–disorder transitions. The order–disorder transition temperature (T_{ODT}) of 500 nm thick poly(α -methylstyrene-*block*-isoprene) films is determined by this technique. Atomic force microscopy on quenched samples is used to verify our conclusion. Disorder and ordering dynamics of these films were examined in real time as the films were heated and cooled across the T_{ODT} . Our work opens the door for using depolarized light scattering for locating transitions between optically isotropic and optically anisotropic block copolymer phases in thin films.

Introduction

Block copolymer thin films have many potential applications, particularly in the field of nanometer-scale lithography for the fabrication of devices such as flash memory and magnetic data storage.^{1–6} These applications require varying degrees of control over the lateral grain structure within the film. This, in turn, has led to a great deal of research related to control and alignment of ordered grains in these materials.^{7–10} The primary means of characterizing thin film grain structure is microscopy, in the form of scanning force microscopy, scanning electron microscopy, and transmission electron microscopy. These techniques are useful but all share a major weakness—they can collect images only on the order of a few square microns in area without losing the resolution necessary to identify and characterize grains.^{11–13} In order to get a single statistically significant snapshot of the state of order in a film, a large number of micrographs are required. This difficulty can be overcome by making measurements in reciprocal space wherein the statistical properties of the entire sample are obtained in one measurement. This paper is part of a series on the development of a new reciprocal space optical method for characterizing the order in block copolymer thin films called guided wave depolarized light scattering (GWDLS).^{14,15} GWDLS, along with grazing incidence small-angle X-ray scattering^{16,17} and resonant soft X-ray scattering,¹⁸ is part of an emerging set of scattering tools geared toward quantifying lateral order in block copolymer thin films. The first experimental results obtained with this technique were reported in ref 14. This was followed by the development of a theoretical model that quantitatively related the GWDLS signal to the morphology of the thin film in ref 15.

GWDLS is based on the depolarized light scattering (DLS) methodology, a widely used technique for characterizing the

morphology of block copolymer films with thicknesses on the order of 1 μm . The main difference is that, in principle, GWDLS can be applied to arbitrarily thin films. As is the case with DLS, a laser beam is aimed through a sample placed between two crossed polarizers, and a photodiode is used to measure the intensity of light leaking through the second polarizer (also known as the analyzer). An isotropic sample (e.g., a disordered phase) or one that is composed of optically isotropic grains (e.g., a gyroid or spheres arranged on a BCC lattice) will not affect the polarization of the light passing through it, resulting in zero signal. A sample composed of optically anisotropic grains (e.g., lamellae or cylinders arranged on a hexagonal lattice) will change the polarization of light passing through it, resulting in a finite signal. If the entire DLS signal is captured, it can be used to quantify the grain structure in bulk block copolymer samples.¹⁹ However, many users of DLS employ it to determine the temperature (or pressure) at which a transition from an optically anisotropic to optically isotropic structure takes place.^{20–22} In such cases, measuring an unspecified portion of the DLS signal is adequate. This is because a finite signal obtained from the anisotropic phase vanishes when the isotropic phase is obtained. Collecting just a portion of the signal (e.g., the signal in the forward direction) affects only the signal-to-noise ratio of the measurement, not the measured phase transition temperature. Because of the extreme precision with which polarization changes of light beams can be measured, very subtle transitions in local structure can be measured by DLS. DLS has, for example, been used to identify the transition between cubic and noncubic network phases that are otherwise very similar²³ and from a weakly ordered lamellar phase to a disordered phase formed in concentrated solutions of randomly grafted copolymers.²⁴

The main purpose of this paper is to report the first measurements of the GWDLS signal from a block copolymer thin film in the vicinity of the order–disorder transition. The top and bottom faces of the thin film are “covered” by low refractive index materials, enabling the sample to act as a waveguide when the light is properly coupled into the film. In an earlier paper, we accomplished this using prisms to couple light into and out of block copolymer films deposited on fused

* Corresponding author.

[†] University of California, Berkeley.

[‡] Department of Chemical and Biological Sciences, Polytechnic University.

[§] Othmer-Jacobs Department of Chemical and Biological Engineering, Polytechnic University.

^{||} Department of Electrical Engineering, Polytechnic University.

[⊥] Lawrence Berkeley National Laboratory.

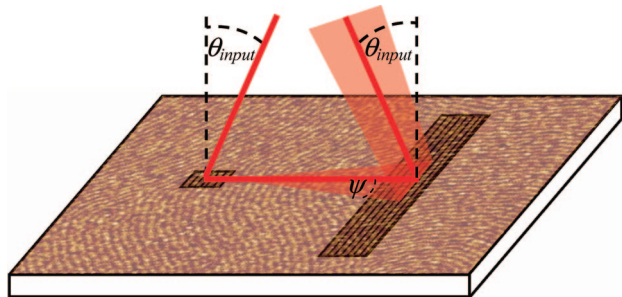


Figure 1. Schematic of light coupling into a film deposited on the grating substrate (left-hand side), propagating laterally through the film while fanning out through angular scattering, and coupling out of the film at the output coupler (right-hand side). In this picture, the gratings and film are on the bottom surface of a transparent substrate, and the light travels through the substrate before encountering the grating.

silica substrates. Coupling was accomplished by pressing the substrate and film assembly against the prisms using pistons with 11 mm diameter round caps. The pistons deformed the substrate and film, reducing the air gap between film and prism until it was small enough for optical tunneling to occur.^{25,26} This technique can only be used to study glassy block copolymers, as the applied force required for coupling would lead to significant distortion of the morphology around the coupling points in rubbery and semicrystalline materials. Likewise, in the case of disordered block copolymers, which are liquids, the sample simply flows away from the coupling points. To circumvent this problem, we have replaced the prism and piston combination with diffraction grating couplers. Diffraction gratings are etched into fused silica substrates upon which the block copolymer thin film is deposited. The light is coupled in and out of the film through the substrate without the application of force. This enables a study of block copolymer thin films both above and below the order–disorder transition temperature (T_{ODT}). Additionally, while position space techniques have been used to study dynamic processes in block copolymer thin films,²⁷ reciprocal space techniques are better suited for such studies. We show that the dynamics of order–disorder transitions can be studied by time-resolved GWDLS with grating couplers. A limitation of grating couplers is that only a small fraction of the total GWDLS signal can be detected. In its present form, GWDLS with grating couplers can thus only be used to track the appearance and disappearance of anisotropic phases in block copolymer thin films, not to quantify the absolute size of the ordered grains therein.

Experimental Section

The experiments described in this paper were primarily performed on an anionically synthesized poly(α -methylstyrene-*block*-isoprene) copolymer (MSI) that was described in a previous publication.¹⁴ The total molecular weight of the MSI polymer was determined as 32 kg/mol. The volume fraction of the poly(α -methylstyrene) block is 0.20, so the expected morphology in the ordered state is hexagonally packed cylinders of poly(α -methylstyrene) in a polyisoprene matrix, which has been confirmed with small-angle X-ray scattering experiments. The order–disorder transition temperature of an MSI polymer bulk sample is $190 \pm 5^\circ\text{C}$, and the bulk glass transition temperature is 150°C . The polydispersity of this polymer is 1.03 as measured by gel permeation chromatography, and the molar percentage of 3–4 isoprene units was 72% as measured by NMR. The refractive indices of poly(α -methylstyrene) and polyisoprene at room temperature are 1.59 and 1.52, respectively.²⁸

The diffraction gratings were etched by Ibsen Photonics in Farum, Denmark, into $25 \times 30 \times 2$ mm fused silica substrates. The substrates thus obtained are shown schematically in Figure 1. A 1×1 mm input coupling grating and a 2×10 mm output

coupling grating were etched into the surface of the fused silica, separated by 10 mm. The output coupler covers a much larger area so that scattered light can exit the film. Each coupler consists of an array of parallel trenches with a rectangular cross section, a period of $\Lambda = 350$ nm, and a depth of 460 nm. The choice of grating geometry will be explained in the Instrument Configuration and Design section. Substrates were soaked in tetrahydrofuran overnight, allowed to dry, and then immersed for 20 min in a piranha solution prepared from a 3:1 volume ratio of concentrated sulfuric acid and hydrogen peroxide to remove remaining organic matter from the substrate surface and grating trenches. Substrates were then removed from the piranha solution and rinsed with deionized water for 30 min and placed gratings-up on a spin-coater and spun at 3000 rpm for 30 s. Substrates were rinsed and spun-dry two more times, once with THF and once with toluene. Finally, an 8 wt % solution of MSI polymer dissolved in toluene was deposited onto the substrates, which were then spun at 3000 rpm for 20 s to give a 500 nm thick polymer film. The samples were placed in an oven and heated to 150°C in a vacuum for 12 h to drive off remaining solvent and ensure wetting of gratings. The resulting block copolymer thin film/substrate composite was clamped into the sample stage of the GWDLS apparatus discussed below.

The GWDLS apparatus is shown schematically in Figure 2. The photon source is a helium–neon laser producing a plane-polarized beam of light with wavelength $\lambda = 633$ nm. The beam passes through a half-wave plate and then through an optical chopper system controlled by a Stanford Research Systems SR540 optical chopper controller and an SR510 lock-in amplifier. The system's chopping frequency is set to 230 Hz, all signal filters are engaged, the two post demodulator low pass filter time constants are set to 10 and 1 s during measurements, and the phase is tuned to maximize the detected signal. After the chopper, the beam passes through a variable neutral density filter followed by a series of beam steering mirrors, an iris, and a Glan-Thompson polarizer. The polarized beam thus obtained enters the sample chamber through a 5×5 mm aperture. The chamber is closed and flooded with argon to reduce polymer degradation at high temperatures. The beam passes through a 5 mm wide by 25 mm tall vertical aperture and is then directed onto the input grating coupler of the fused silica substrate, which is oriented in the vertical plane with respect to the table. The majority of the incident beam does not couple into the film. It is either reflected off the surface of the substrate or transmitted through both the substrate and the film. The reflected beam is blocked by the back of the plate with the 5×25 mm vertical aperture, and the transmitted beam encounters a beam dump. The angle and position of the substrate in relation to the beam must be very precisely controlled to allow the film to function as a waveguide, and accordingly the substrate is mounted on a stage with angular control (with 0.3 mrad precision) and three axes of translational control (with $10\ \mu\text{m}$ precision on each axis). The sample holder contains two heating elements that are controlled by an Omega CN9000A temperature controller. A thermocouple mounted on the sample stage is used to control the sample temperature. When the sample is positioned properly, a small fraction of the incident light is guided through 1 cm of the block copolymer thin film, after which it is coupled out of the film by the output coupler. The exiting beam passes through an analyzing polarizer built into the side of the sample chamber. The light then passes through a 1 mm tall 7 cm wide horizontal slit mounted on a vertical translational stage, which selects a specific scattering angle, ψ , defined in Figure 1. The light then passes through a 1 mm wide 2 cm tall vertical slit that blocks incoming light that is not at the output coupling angle of the waveguide (θ_{input} in Figure 1). Finally, the light encounters the photodiode detector, which is connected to the SR510 lock-in amplifier. The photodiode and vertical slit are both mounted on a rail atop a horizontal translational stage, which allows the measurement of intensity as a function of the output coupling angle.

Our GWDLS experiments were conducted on 500 nm thick films at temperatures between 25 and 200°C . Our attempts to study films

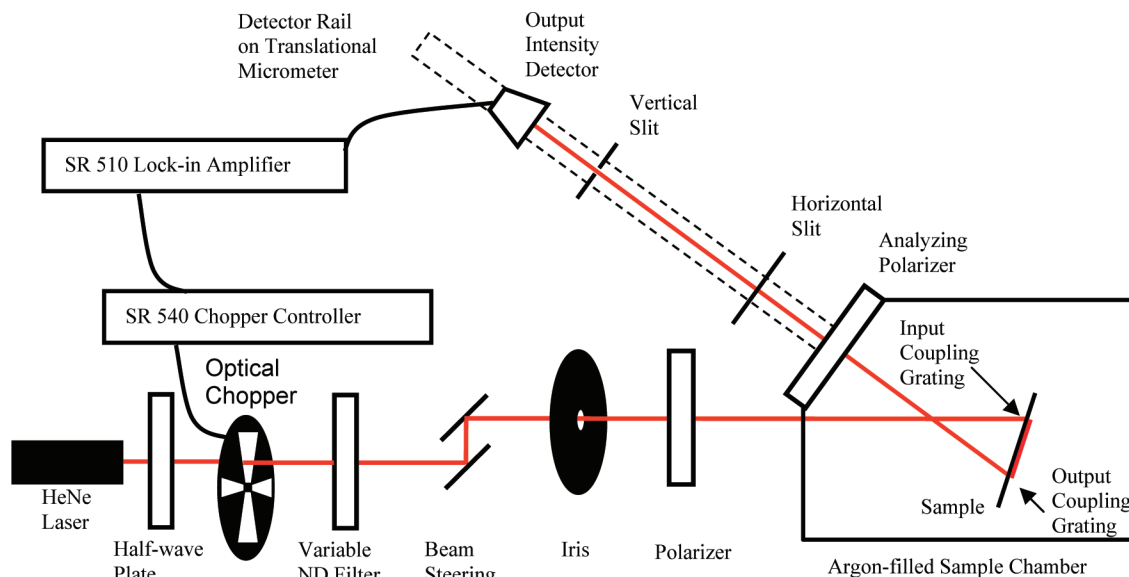


Figure 2. Diagram of the GWDLS apparatus.

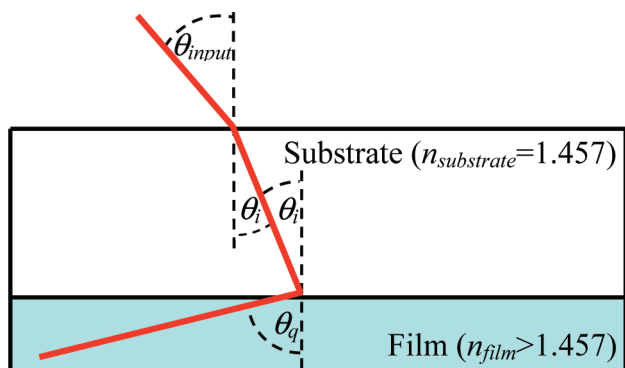


Figure 3. Schematic of light coupling into a film via a diffraction grating coupler.

with thicknesses less than 500 nm were thwarted by dewetting, as were our attempts to heat our films above 200 °C.

The effect of temperature on grain structure in 500 nm thick MSI films was verified using atomic force microscopy (AFM). For this verification, films were prepared as above, but on silicon substrates appropriate for use in our AFM instead of the large fused silica substrates used for GWDLS. Annealing was performed in a vacuum oven, and samples were cooled to room temperature before they were imaged. Images were captured using a Digital Instruments Multimode AFM and NanoScope IIIa controller operated in tapping mode. Nanosensors NCL-50 Pointprobe tips were autotuned to frequencies near 147 kHz and drive amplitudes below 100 mV using Digital Instruments NanoScope Control software. All micrographs in this publication are phase-contrast AFM images.

Instrument Configuration and Design

Figure 3 is a schematic showing both the incident and coupled light beams in the vicinity of the substrate and block copolymer film, where $n_{\text{substrate}}$ and n_{film} are the indices of refraction of the substrate and film, θ_{input} is the angle between the incoming laser beam and a normal to the substrate surface and is also equal to the output coupling angle, as seen in Figure 1, θ_i is the angle between the direction of propagation of light inside the substrate and a normal to the substrate surface, and θ_q is the angle between the direction of propagation of light inside the film and a normal to the film surface. For a given film thickness and index of refraction, and for a substrate index of refraction, the wave guiding angles are quantized and well-defined.²⁹ Since the index

of refraction of typical block copolymer films ($n_{\text{film}} = 1.5\text{--}1.7$) and of the substrate ($n_{\text{substrate}} = 1.457$) are similar, transmission modes are expected to be more efficient for coupling than are reflection modes. We therefore use the grating in the transmission mode as shown in Figure 3.

For design purposes we assume that we have a 500 nm thick block copolymer film with $n_{\text{film}} = 1.54$ on a fused silica substrate. Such a film guides a single transverse electric or transverse magnetic wave from our $\lambda = 633$ nm laser at $\theta_q = 75^\circ$. Using the diffraction equation

$$n_{\text{film}} \sin \theta_q = n_{\text{substrate}} \sin \theta_i - q \left(\frac{\lambda}{\Lambda} \right) \quad (1)$$

where θ_q is the diffracted beam angle, θ_i is the incident beam angle, q is the diffracted order number ($0, \pm 1, \pm 2, \dots$), and Λ is the period of the grating, one can determine the angle of the incident beam required for wave guiding with a particular grating geometry.³⁰ Using Snell's law and eq 1, the required external angle for coupling is thus

$$\theta_{\text{input}} = \arcsin \left\{ \left(\frac{n_{\text{substrate}}}{n_{\text{air}}} \right) \left[\left(\frac{n_{\text{film}}}{n_{\text{substrate}}} \right) \sin \theta_q + \left(\frac{q}{n_{\text{substrate}}} \right) \left(\frac{\lambda}{\Lambda} \right) \right] \right\} \quad (2)$$

Additionally, one can determine the number of diffracted modes supported by a given grating and angle pair from eq 1 because only q values for which

$$\left| \frac{n_{\text{substrate}} \sin \theta_i - q \left(\frac{\lambda}{\Lambda} \right)}{n_{\text{film}}} \right| \leq 1 \quad (3)$$

produce noncomplex, physically meaningful angles θ_q .

The intensity of the coupled light is maximized when only one mode is coupled into the film, i.e., when there is only one nonzero value of q consistent with eq 3. This is facilitated by a small value of Λ . We chose $\Lambda = 350$ nm as a compromise between ease of manufacturing (small features are more difficult and expensive to fabricate) and efficiency of coupling (gratings with larger Λ couple at θ_i angles near zero, which leads to a strong Bragg reflection and decreased transmission coupling efficiency). For $\Lambda = 350$ nm, θ_i is 12.71° . The ideal grating trench depth is dependent on the index of refraction and thickness of the film deposited onto it.²⁹ For films of interest to us, this value ranges from 400 to 600 nm. We chose a depth of

460 nm. A series of 460 nm deep rectangular trenches with $\Lambda = 350$ nm were used as both input and output couplers in the orientation shown in Figure 1. Blazed gratings with angled features may be used in the future to improve signal strength but were not used here due to fabrication cost considerations.

The procedure for a GWDLS experiment with grating couplers is substantially different from that used for GWDLS with prism couplers described in a previous publication.¹⁴ We therefore outline all of the experimental steps here. The substrate was clamped to the heated sample mount with the side supporting the block copolymer film facing away from the laser for transmission coupling as in Figure 3. The half-wave plate and Glan-Thompson polarizer were adjusted so that the incident beam was polarized in the vertical, transverse electric (TE) plane, the optical chopper and lock-in amplifier were activated, and the sample translational and rotational micrometers were adjusted to locate the input coupling position and angle needed for waveguiding through the block copolymer film. The detector was placed at the angle needed to intercept the beam of light coupled out at $\psi = 0$. The position and angle of the sample were adjusted to maximize the detected intensity of light. The analyzing polarizer was rotated to the TE polarization plane. The detector rail was then translated perpendicularly to the direction of propagation of the output beam, and measurements were taken as a function of the output coupling angle (θ_{input} in Figure 1). The intensity far from the output beam in both directions was averaged and defined as a background and then subtracted from the peak intensity. The resulting background-subtracted peak intensity is defined as S_{TE} . The analyzing polarizer was then rotated to the transverse magnetic (TM) polarization plane, and the detector rail was again translated to take measurements of the intensity of depolarized light and of the background on either side of the peak. The resulting background-subtracted depolarized peak intensity is S_{TM} . The normalized depolarized signal I is defined

$$I = \frac{S_{\text{TM}}}{S_{\text{TE}}} \quad (4)$$

To perform a temperature-scan experiment, argon flow through the sample chamber began 30 min before heating above room temperature. After an initial GWDLS measurement was taken at room temperature, the sample temperature was adjusted to the desired level. For temperature scans, the temperature was held for at least 30 min to allow the signal to stabilize before measurements were performed. At each temperature the angle of the rotational stage had to be slightly altered to restore coupling due to the change in refractive index of the film on heating. After rotating the sample stage to maximize the output-coupled TE intensity, the TE and TM signals were measured as described above.

It must be noted that the grating couplers are themselves birefringent, with optical anisotropy that is characterized by the difference between their extraordinary and ordinary refractive indices

$$\Delta n = n_e - n_o \quad (5)$$

where n_e and n_o are the refractive indices of light polarized perpendicular and parallel to the optic axis, respectively. The optic axis is identical to the propagation direction at $\psi = 0$ inside the film in Figure 1. These values can be calculated from

$$n_e^2 - n_o^2 = \frac{\phi_{\text{trench}}\phi_{\text{grating}}(n_{\text{trench}}^2 - n_{\text{grating}}^2)^2}{\phi_{\text{trench}}n_{\text{grating}}^2 + \phi_{\text{grating}}n_{\text{trench}}^2} \quad (6)$$

and

$$n_o = \sqrt{\phi_{\text{trench}}n_{\text{trench}}^2 + \phi_{\text{grating}}n_{\text{grating}}^2} \quad (7)$$

where ϕ_{trench} is the volume fraction of the grating composed of etched trenches, ϕ_{grating} is the volume fraction of the grating

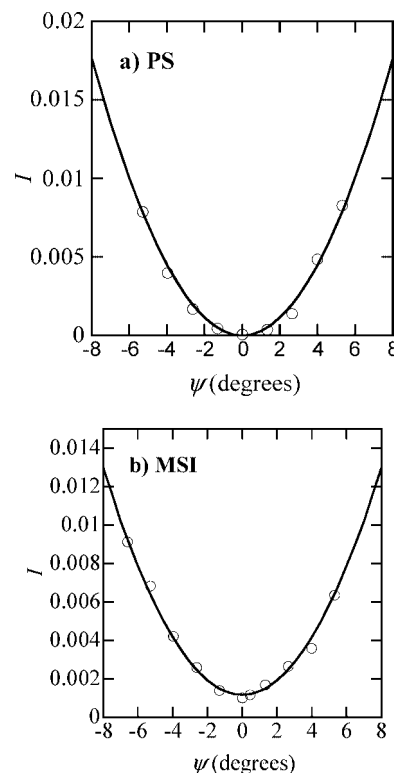


Figure 4. Experimental data (open circles) accompanied by theoretical predictions (solid lines) showing the dependence of the measured depolarized signal, I , on the angle ψ for (a) a typical 500 nm polystyrene homopolymer film and (b) a typical 500 nm poly(α -methylstyrene-block-isoprene) copolymer film.

composed of fused silica ridges, n_{trench} is the refractive index of the polymer or air in the trench, and n_{grating} is the refractive index of fused silica. ϕ_{trench} and ϕ_{grating} are both ~ 0.5 , n_{grating} is 1.457, and n_{trench} is the refractive index of the material in the trench. For a beam that spreads uniformly as depicted in Figure 1, the depolarized signal due to the presence of the grating is given by

$$I = A \sin^2 2\psi \quad (8)$$

where

$$A = \left(\frac{\pi \Delta n l}{\lambda} \right)^2 \sin^4(90^\circ - \theta_i) \quad (9)$$

and l is the interaction path length between the light and the crystal.¹⁹ The grating contribution to the detected signal is zero only when $\psi = 0$. Experimental $I(\psi)$ results obtained from a 500 nm thick polystyrene film are shown in Figure 4a. The curve through the data is a least-squares fit of eq 8 with A as an adjustable parameter. The fit gives $A = (2.33 \pm 0.07) \times 10^{-1}$. The value of Δn obtained from the fitted value of A and eq 9 is 1.51×10^{-1} , which is higher than the expected Δn value for trenches completely filled with air ($n_{\text{trench}} = 1.00$ and $\Delta n = 8.36 \times 10^{-2}$) or with polystyrene ($n_{\text{trench}} = 1.59$ and $\Delta n = 5.89 \times 10^{-3}$). The most likely cause of this discrepancy is partial filling of the grating coupler's trenches with polymer, which is not unreasonable given the processing history of the films. Partial filling of a diffraction grating is expected to enhance form birefringence above the values predicted by eqs 5–7, leading to a Δn value higher than that of a grating with trenches completely full of air or polymer.³¹ It is worth noting that $I(\psi=0) = 0$ for the PS film.

In Figure 4b we show $I(\psi)$ data obtained from a 500 nm thick MSI film. The data are similar to those obtained from the

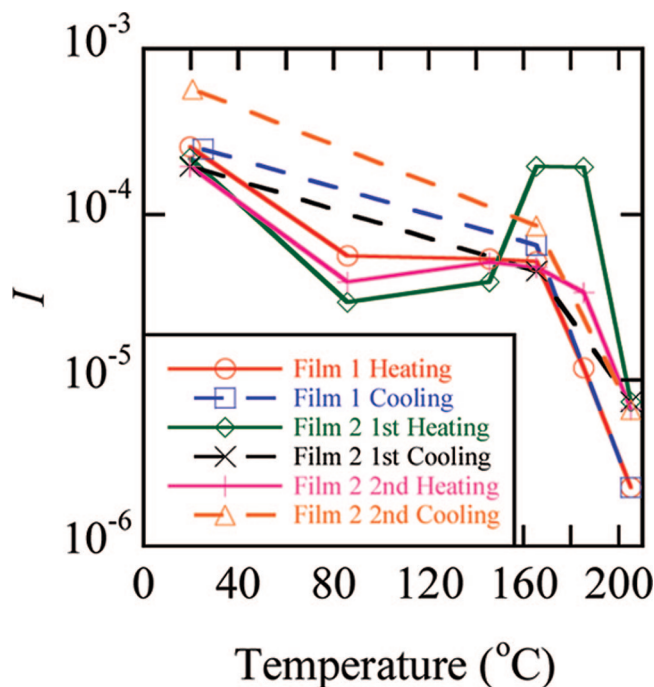


Figure 5. Typical temperature dependence of the normalized depolarized signal, I , of 500 nm MSI films as they are heated above the bulk T_{ODT} and subsequently cooled below it. Film 1 went through one such cycle, and film 2 went through two cycles.

polystyrene film except for the fact that $I(\psi=0)$ is finite. The curve in Figure 4b is a fit to the equation

$$I = A \sin^2 2\psi + B \quad (10)$$

with A and B as adjustable parameters. The fitted value of A for the MSI film is $(1.55 \pm 0.05) \times 10^{-1}$, which is similar to that obtained from the polystyrene film. The associated Δn value for the grating coupler calculated using eq 9 is 1.26×10^{-1} , which is again higher than that expected for gratings filled with air ($n_{\text{trench}} = 1.00$ and $\Delta n = 8.36 \times 10^{-2}$) or with MSI polymer ($n_{\text{trench}} = 1.54$ and $\Delta n = 2.30 \times 10^{-3}$). As with the polystyrene films, the cause of the discrepancy in Δn is believed to be partial filling of the grating trenches with polymer. The value of B obtained from the fit is $(1.16 \pm 0.11) \times 10^{-3}$. This value represents the GWDLS signal generated by optically anisotropic grains in the block copolymer sample instead of by the output grating coupler.

The angular spreading of the light away from $\psi = 0$ as it propagates through the waveguide is caused by interactions with surface imperfections in the film.²⁵ At nonzero ψ angles the grating coupler produces a significant depolarized signal unrelated to the grain structure of the film. In the vicinity of $\psi = 0$ the depolarized signal from the grating coupler disappears, and the measured signal is due only to the presence of ordered grains within the film. Thus, all of the subsequent experiments were performed with the horizontal slit adjusted to be centered on $\psi = 0$. At this position, the detected angular range is $-0.19^\circ < \psi < 0.19^\circ$, over which the normalized depolarized signal of PS films was $(1.8 \pm 1.1) \times 10^{-5}$ and from ordered MSI films was $(6.5 \pm 4.6) \times 10^{-4}$.

Scattering Results and Discussion

Temperature-scan experiments were performed on MSI films in which the temperature was raised in a series of steps from room temperature to 205 °C and then lowered to 165 °C for an extended anneal. While the absolute values of the initial

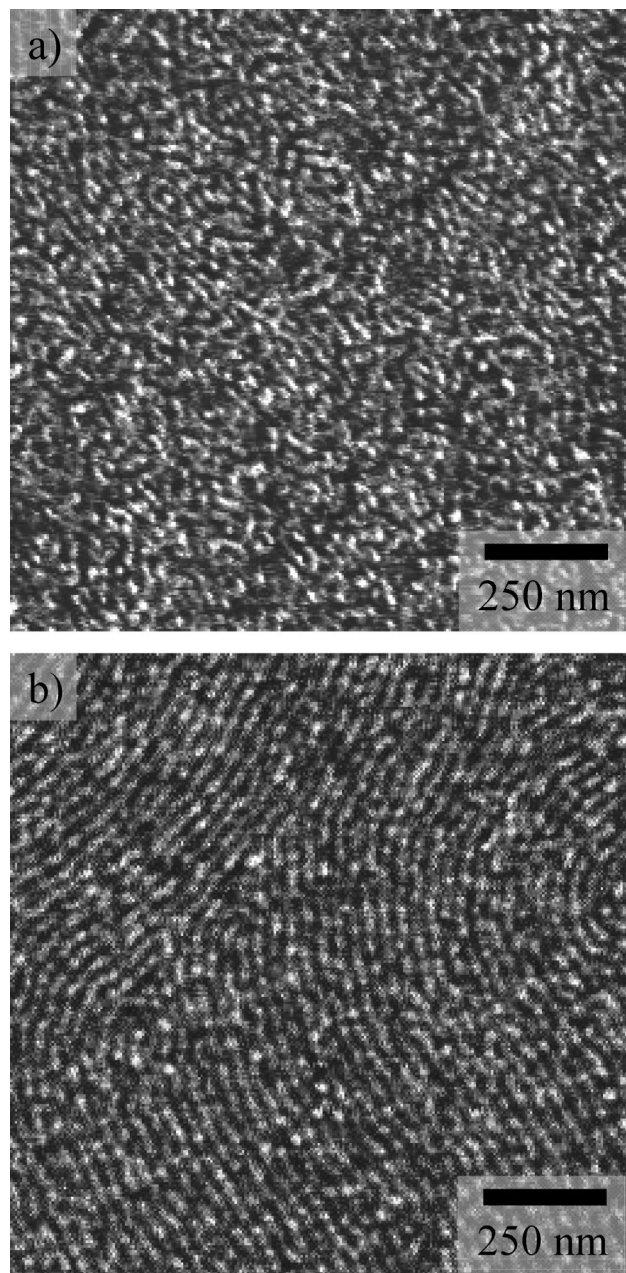


Figure 6. Typical phase images obtained by AFM on 500 nm thick MSI films showing (a) the absence of long-range order in films heated to 205 °C and then quenched quickly to room temperature (phase range = 15°) and (b) the ordered grain structure present in films heated to 205 °C, cooled to 165 °C, and annealed for 4 h before quenching to room temperature (phase range = 10°).

normalized depolarized signal varied from film to film, the change in the signal in response to temperature increases from 20 to 205 °C was qualitatively similar. Figure 5 shows the typical temperature dependence of the depolarized signal for MSI films. The value of I , which is about 3×10^{-4} at room temperature, generally decreases with increasing temperature. At 205 °C, the highest temperature used in our experiments, the value of I is in the vicinity of 1×10^{-5} , comparable to the signal obtained from the PS sample. We conclude that our MSI films were disordered at 205 °C. The T_{ODT} of the 500 nm thick MSI films is thus 195 ± 10 °C, which is very close to the 190 ± 5 °C value for bulk MSI. On the basis of previous studies on the effect of film thickness on T_{ODT} , we do not expect the T_{ODT} of a 500 nm thick MSI film to be substantially different from that of the bulk sample.³² After disordering, cooling the sample

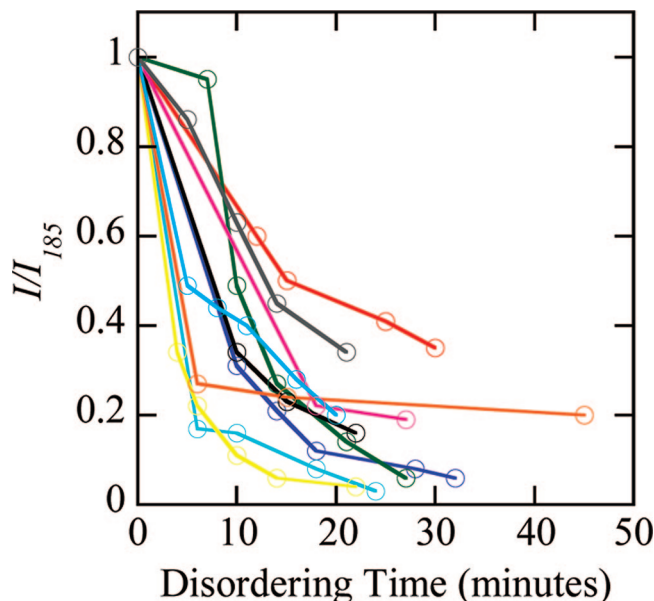


Figure 7. Dynamics of the order-to-disorder transition in block copolymer thin films. The depolarized signal, I , is normalized by its value at 185 °C. Time zero is defined as the time at which the temperature controller setting was switched from 185 to 205 °C. It takes about 3 min for the film temperature to reach 205 °C after the switch. Experimental data obtained from 10 independent runs are shown.

to 165 °C and below led to an increase in I to values that were similar to those obtained during the heating scan. As seen in Figure 5, repeated heating and cooling scans with different films and repeated scans on the same film gave similar results.

In order to verify this behavior, similar MSI films were deposited on silicon substrates, heated to 205 °C under vacuum, and then quenched to room temperature over the course of 2 min in order to preserve grain structure. These films were then imaged using AFM. As seen in the typical image shown in Figure 6a, these films exhibited no signs of long-range order, confirming that MSI films are disordered on heating to 205 °C. Additional films were prepared by disordering at 205 °C for 30 min and then cooling to 165 °C and annealing for 4 h before the samples were quenched to room temperature and imaged in AFM. As seen in the representative image shown in Figure 6b, this temperature profile resulted in significant grain growth in MSI films, agreeing with the increase in the depolarized signal seen in GWDLS during annealing at 165 °C after disordering.

In Figure 7 we show the time dependence of I after a step change in temperature from 185 to 205 °C. We show data obtained from 10 different films. The value of I obtained in the ordered state varied from sample to sample. To account for this, we normalized $I(t)$ by I obtained at 185 °C immediately prior to heating to 205 °C. We see that in all of the samples I decays monotonically with a time constant of about 30 min. The rapidly diminishing depolarized scattering encountered upon crossing the bulk T_{ODT} value is similar to disordering data presented in the original papers introducing depolarized light scattering as a technique for tracking order–disorder transitions in bulk samples.^{19,33}

The time dependence of I upon lowering the temperature from 205 to 165 °C is shown in Figure 8. The time-resolved signals obtained from MSI films during the disorder-to-order transition (Figure 8) are much more varied than those obtained during the order-to-disorder transition (Figure 7). This is similar to data from our early studies of bulk block copolymers, in which the depolarized signal obtained in the ordered state varied considerably from run to run.³³ Obtaining reproducible signals from bulk samples of ordered block copolymers requires extremely careful

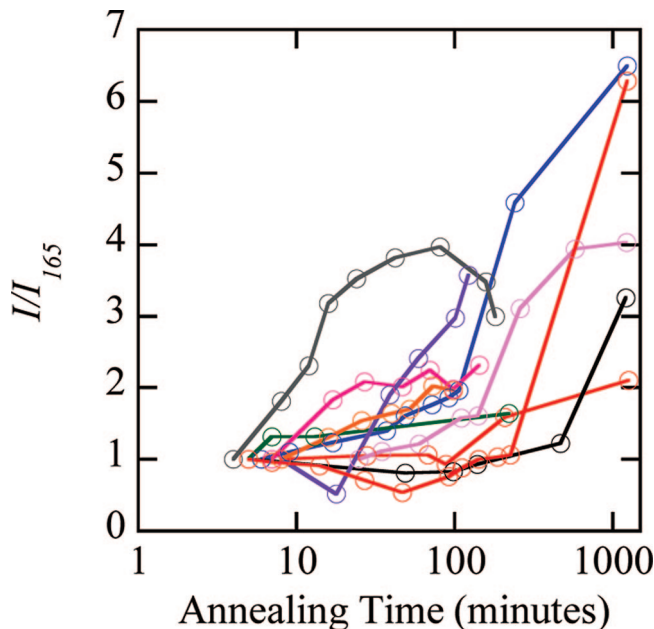


Figure 8. Dynamics of the disorder-to-order transition in block copolymer thin films. The depolarized signal, I , is normalized by its first value at 165 °C after cooling from 205 °C. Time zero is defined as the time at which the temperature controller setting was switched from 205 to 165 °C. It takes about 5 min for the film temperature to reach 165 °C after the switch. Experimental data obtained from 10 independent runs are shown.

control over thermal history. We note that precise control over the temperature of a thin film with one face exposed to flowing argon will require a much more sophisticated apparatus than the one used in this study.

Conclusions

We have demonstrated that guided wave depolarized light scattering with diffraction grating couplers etched into fused silica substrates can be used to study soft block copolymer films in the vicinity of order–disorder transitions. The diffraction gratings can only be used to detect depolarized light along the original propagation direction of the guided wave. This enables the detection of the order–disorder transition temperature of 500 nm thick MSI films. Our work opens the door for studying order–order transitions between optically isotropic and optically anisotropic block copolymer phases in thin films. Collecting only a portion of the depolarized light scattering signal eliminates the possibility of analyzing the angular dependence of depolarized scattering from the film, which would otherwise be a source of more grain structure information.¹⁵ Given that the light scattered from the TE polarization to the TM polarization by the film will couple out of the film at the TM coupling angle, while the light scattered from the TE polarization to the TM polarization by the diffraction grating will have already exited the film and appear at the TE coupling angle, a high-resolution 2-D CCD camera positioned on the detector arm may allow decoupling of the film-scattered and grating-scattered effects. While there is considerable room for improvements, we believe that the present work establishes a new technique for studying phase transitions in block copolymer thin films.

Acknowledgment. Financial support was provided by the National Science Foundation (DMR-0514422).

References and Notes

- (1) Park, M.; Harrison, C.; Chaikin, P. M.; Register, R. A.; Adamson, D. H. *Science* **1997**, 276, 1401–1404.

- (2) Cheng, J. Y. R.; , C. A.; Chan, V. Z.-H.; Thomas, E. L.; Lammertink, R. G. H.; Vancso, G. J. *Adv. Mater.* **2001**, *13*, 1174–1178.
- (3) Cheng, J. Y.; Ross, C. A.; Thomas, E. L.; Smith, H. I.; Vancso, G. J. *Appl. Phys. Lett.* **2002**, *81*, 3657–3659.
- (4) Cheng, J. Y. R.; , C. A.; Thomas, E. L.; Smith, H. I.; Vancso, G. J. *Adv. Mater.* **2003**, *15*, 1599–1602.
- (5) Mansky, P.; Liu, Y.; Huang, E.; Russell, T. P.; Hawker, C. *Science* **1997**, *275*, 1458–1460.
- (6) Naito, K.; Hieda, H.; Sakurai, M.; Kamata, Y.; Asakawa, K. *IEEE Trans. Magn.* **2002**, *38*, 1949–1951.
- (7) Segalman, R. A. *Mater. Sci. Eng., R* **2005**, *48*, 191–226.
- (8) Segalman, R. A.; Yokoyama, H.; Kramer, E. J. *Adv. Mater.* **2001**, *13*, 1152–1155.
- (9) Craig, G. S. W.; Nealey, P. F. J. *Photopolym. Sci. Technol.* **2007**, *20*, 511–517.
- (10) Wilmes, G. M.; Durkee, D. A.; Balsara, N. P.; Liddle, J. A. *Macromolecules* **2006**, *39*, 2435–2437.
- (11) Fasolka, M. J.; Mayes, A. M. *Annu. Rev. Mater. Res.* **2001**, *31*, 323–355.
- (12) Angelescu, D. E.; Harrison, C. K.; Trawick, M. L.; Chaikin, P. M.; Register, R. A.; Adamson, D. H. *Appl. Phys. A* **2004**, *78*, 387–392.
- (13) Hexemer, A.; Stein, G. E.; Kramer, E. J.; Magonov, S. *Macromolecules* **2005**, *38*, 7083–7089.
- (14) Garetz, B. A.; Newstein, M. C.; Wilbur, J. D.; Patel, A. J.; Durkee, D. A.; Segalman, R. A.; Liddle, J. A.; Balsara, N. P. *Macromolecules* **2005**, *38*, 4282–4288.
- (15) Fang, Z.; Newstein, M. C.; Garetz, B. A.; Wilbur, J. D.; Balsara, N. P. *J. Opt. Soc. Am. B* **2007**, *24*, 1291–1297.
- (16) Muller-Buschbaum, P. *Anal. Bioanal. Chem.* **2003**, *376*, 3–10.
- (17) Lee, B.; Park, I.; Park, S.; Yoon, J.; Kim, J.; Kim, K.-W.; Chang, T.; Ree, M. *Macromolecules* **2005**, *38*, 4311–4323.
- (18) Virgili, J. M.; Tao, Y.; Kortright, J. B.; Balsara, N. P.; Segalman, R. A. *Macromolecules* **2007**, *40*, 2092–2099.
- (19) Balsara, N. P.; Garetz, B. A.; Dai, H. J. *Macromolecules* **1992**, *25*, 6072–6074.
- (20) Migler, K. B.; Han, C. C. *Macromolecules* **1998**, *31*, 360–365.
- (21) Epps, T. H.; Cochran, E. W.; Bailey, T. S.; Waletzko, R. S.; Hardy, C. M.; Bates, F. S. *Macromolecules* **2004**, *37*, 8325–8341.
- (22) Zryd, J. L.; Burghardt, W. R. *Macromolecules* **1998**, *31*, 3656–3670.
- (23) Chatterjee, J.; Jain, S.; Bates, F. S. *Macromolecules* **2007**, *40*, 2882–2896.
- (24) Eitouni, H. B.; Rappl, T. J.; Gomez, E. D.; Balsara, N. P.; Qi, S.; Chakraborty, A. K.; Frechet, J. M. J.; Pople, J. A. *Macromolecules* **2004**, *37*, 8487–8490.
- (25) Tien, P. K. *Appl. Opt.* **1971**, *10*, 2395.
- (26) Ulrich, R.; Torge, R. *Appl. Opt.* **1973**, *12*, 2901–2908.
- (27) Harrison, C.; Adamson, D. H.; Cheng, Z. D.; Sebastian, J. M.; Sethuraman, S.; Huse, D. A.; Register, R. A.; Chaikin, P. M. *Science* **2000**, *290*, 1558–1560.
- (28) Bicerano, J. *Prediction of Polymer Properties*; Marcel Dekker: New York, 1993.
- (29) Tamir, T.; Peng, S. T. *Appl. Phys.* **1977**, *14*, 235–254.
- (30) Hecht, E. *Optics*, 4th ed.; Addison-Wesley: Reading, MA, 2002.
- (31) Thornburg, W. J. *Cell Biol.* **1957**, *3*, 413–419.
- (32) Alexander-Katz, A.; Fredrickson, G. H. *Macromolecules* **2007**, *40*, 4075–4087.
- (33) Balsara, N. P.; Perahia, D.; Safinya, C. R.; Tirrell, M.; Lodge, T. P. *Macromolecules* **1992**, *25*, 3896–3901.

MA702587U